PSK Error Performance with Gaussian Noise and Interference

By ARNOLD S. ROSENBAUM

(Manuscript received September 13, 1968)

A single, constant amplitude, in-band, additive interference is included in the analysis of detecting phase shift keyed signals in gaussian noise. For coherent detection we give a method applicable to any M-phase system, and evaluate the symbol error probability for $M = 2$, 3, and 4. For differential detection we treat the important cases $M = 2$, 4, 8, and 16, offering comprehensive numerical results for each.

The analysis in each case is based on a single sinusoid with random phase adding to the noisy phase shift keyed signal. The results are then interpreted to include an angle modulation impressed on the continuous wave interferer. The receiver consists of an ideal phase discriminator with a perfect slicer. The channel is also assumed ideal in that intersymbol interference is not considered.

I. INTRODUCTION

Phase shift keying (psk) is becoming more popular as a modulation scheme for transmitting digital information. Lately much analysis has been done for both coherent and differentially coherent detection. Unfortunately the analyses done to date have generally considered only two signal degradations: channel anomalies (such as distortion, gain and delay variations, and so on) and thermally generated noise modeled by a gaussian random process. This article considers the effects of a spurious signal, or interference, falling in the band of the desired signal, as well as gaussian noise. It is understood that both the noise and the interference additively corrupt the desired signal; these are the only perturbing factors.

For coherent detection, the phase probability density function for the received composite of signal, noise, and interference is found. From this, the theoretical error probability may be evaluated for

any M-phase system. We give comprehensive numerical results for the important cases, $M = 2, 3, 4$.

For differential detection we present analysis and results for $M = 2$, 4, 8, and 16. In the binary case a simple closed form solution was found which yields both a good approximation and exact bounds to the actual error probability. The solutions to the multilevel $M > 2$ differential detection problem, which are exact, required machine computation of a double integral; complete numerical results are given.

Finally, we draw general comparisons between coherent and differential detection error performance as affected by interference.

II. SIGNALS, NOISE, AND INTERFERENCE

A phase shift keyed signal has the form (ignoring any amplitude function)

$$s(t) = \cos [2\pi f_s t + \phi_s(t)] \tag{1}$$

where we choose to normalize the peak signal amplitude to unity. The digital modulation is carried in the angle of s by $\phi_s(t)$, which assumes discrete values from a set of M equally spaced points in $[0, 2\pi]$ at the sample times T seconds apart. Thus the Nth message or baud is modulated by

$$\phi_s(NT) = \frac{2\pi k}{M}, \qquad k = 0, 1, 2, \cdots, M - 1 \tag{2}$$

where each of the M values of k is equally probable.

For a coherent receiver an M-ary symbol is transmitted in one baud by the value of k. For a differential detection receiver the information is transmitted by the changes in k (or carrier phase) between adjacent bauds.

The noise is presumed to originate thermally and is therefore modeled in the usual fashion by a stationary zero mean gaussian random process with uniform spectral density. At the output of a symmetrical bandpass filter the noise voltage may be written as[1]

$$n(t) = u(t) \cos (2\pi f_s t) - v(t) \sin (2\pi f_s t) \tag{3}$$

where u and v are low-pass, stationary, independent, zero mean gaussian random processes with ensemble averages

$$\langle n^2 \rangle_{av} = \langle u^2 \rangle_{av} = \langle v^2 \rangle_{av} = \sigma^2, \tag{4}$$

equal to the noise power.

In the differential detection analysis we make the further restriction that the noise process autocorrelation vanish at the baud interval, thus

$$R_{nn}(T) = 0. \tag{5}$$

This assures the four gaussian random variables

$$u(t_0),\ u(t_0 + T),\ v(t_0),\ v(t_0 + T)$$

to be uncorrelated and hence independent.[2]

Interference shall consist of a constant amplitude, possibly angle modulated, sinusoid which lies within the bandwidth of the detector. It is assumed to originate independently of the signal, and so it is natural that its phase relationship to the signal is random with all angles equally probable. Therefore let

$$i(t) = b \cos [2\pi f_i t + \phi_i(t) + \Gamma] \tag{6}$$

which has a peak value of b, and is angle modulated by ϕ_i. The arbitrary phase angle Γ, independent of ϕ_i, is a random variable whose probability density function is $(2\pi)^{-1}$ when reduced modulo 2π.

For coherent detection, where the interference is observed only once per symbol, the random phase variable Γ vitiates the modulation ϕ_i because the sum $(\phi_i + \Gamma)$ is distributed exactly as if it were uniform. This is discussed in Section III.

III. COHERENT DETECTION

An ideal phase discriminator is assumed which compares the received wave (composed of signal, noise, and interference) with the unmodulated signal carrier (the reference) and produces instantly the signed phase difference between the two inputs.

The detector examines the discriminator output and announces an estimate of the transmitted symbol. The detector operates with no timing error and with zero width decision thresholds. Using maximum likelihood detection based on equal *a priori* symbol probabilities, the thresholds are at π/M, $(3\pi)/M$, . . . , $[(2M - 1)\pi]/M$. In a phasor diagram these thresholds correspond to $(2\pi)/M$ angular sections centered about the M signal positions.

The approach used to find Pe, the probability of a symbol error, is to find the probability density function of the phase of the received composite $(s + n + i)$, and then integrate the density over the error regions.

We first notice that the phase angle of the interference relative to the signal is, from equations (1) and (6),

$$\Phi(t) \equiv 2\pi(f_i - f_s)t + \phi_i(t) - \phi_s(t) + \Gamma \tag{7}$$

where Γ is independent of the other terms on the right-hand side. Since Γ is uniformly distributed modulo 2π, the relative interference phase process $\Phi(t)$ is also uniformly distributed modulo 2π. This is a general result for the modulo addition of several variables, one of which is uniform.[3]

Figure 1 is a phasor diagram of the receiver input components, signal, interference, and noise, at a sample time t_0. The phase reference is $2\pi f_s t + \phi_s$ so that the signal lies along the reference (vertical) axis. The orthogonal noise phasors are assumed to be at angles 0 and $\pi/2$, relative to the signal. We seek the probability density function of the resultant angle A, and begin by considering the two dimensional joint probability density function of the cartesian coordinates of the resultant phasor. Conditioned on Φ, it is clearly jointly gaussian with means

$$\langle x \rangle_{av} = b \sin \Phi, \qquad \langle y \rangle_{av} = 1 + b \cos \Phi \tag{8}$$

so that

$$f_{XY}(x, y \mid \phi) = \frac{1}{2\pi\sigma^2} \exp\left\{-\frac{1}{2\sigma^2}[(x - b\sin\phi)^2 + (y - 1 - b\cos\phi)^2]\right\}. \tag{9}$$

Eliminating the Φ dependency gives

$$f_{XY}(x, y) = \frac{\exp\left\{-\frac{1}{2\sigma^2}[x^2 + (y-1)^2 + b^2]\right\}}{(2\pi\sigma)^2} \cdot \int_0^{2\pi} \exp\left\{\frac{b}{\sigma^2}[x^2 + (y-1)^2]^{\frac{1}{2}} \cos(\phi + \eta)\right\} d\phi \tag{10}$$

where $\eta = \tan^{-1}[(y-1)/x]$ is not a function of ϕ.

This integrates directly to

$$f_{XY}(x, y) = \frac{1}{2\pi\sigma^2} \exp\left\{-\frac{1}{2\sigma^2}[x^2 + (y-1)^2 + b^2]\right\} \cdot I_0\left\{\frac{b}{\sigma^2}[x^2 + (y-1)^2]^{\frac{1}{2}}\right\} \tag{11}$$

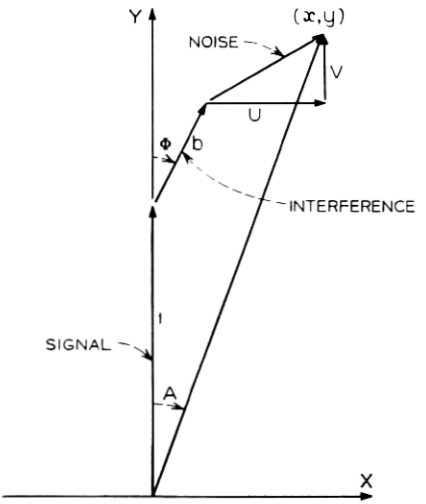

Fig. 1 — Phasor diagram of the signal, noise, and interference components at a sample time t_0.

where I_0 is the zero order modified Bessel function of the first kind.

We now convert equation (18) to polar coordinates through the usual transformation

$$x = r \sin \alpha \quad \text{and} \quad y = r \cos \alpha \tag{12}$$

which has the Jacobian r. Then the polar coordinate two-dimensional density is integrated over all radius values to yield the desired probability density function of the angle.

$$f_A(\alpha) = \frac{1}{2\pi\sigma^2} \int_0^\infty \exp\left\{-\frac{1}{2\sigma^2}[r^2 + b^2 + 1 - 2r\cos\alpha]\right\} \cdot I_0\left[\frac{b}{\sigma^2}(r^2 + 1 - 2r\cos\alpha)^{\frac{1}{2}}\right] r\, dr. \tag{13}$$

The above integration has been done numerically to generate exact $f_A(\alpha)$ curves for several values of

$-20 \log_{10}[2^{\frac{1}{2}}\sigma]$ = carrier to noise ratio in dB (CNR),

$-20 \log_{10} b$ = carrier to interference ratio in dB (CIR).

It is clear from equation (13) that $f_A(\alpha)$ has at least the symmetries of cos α.

Figure 2 offers typical families of f_A probability density function

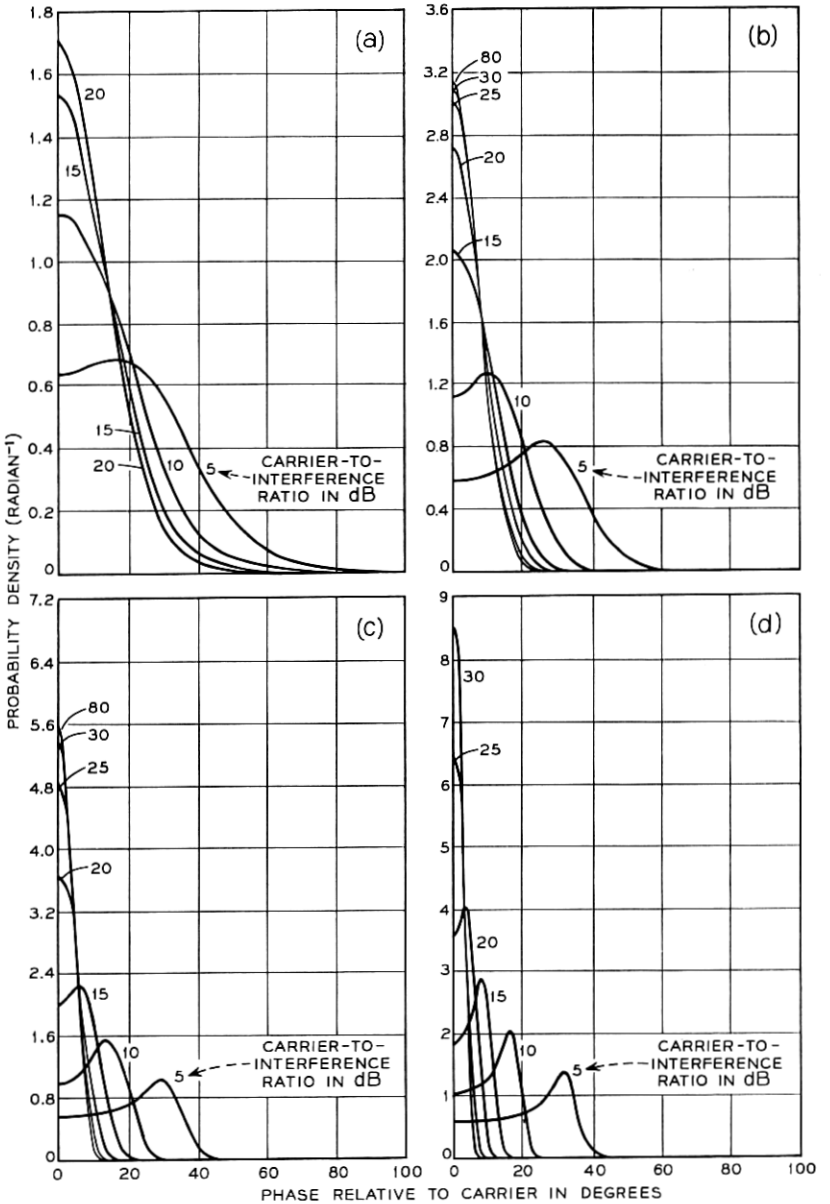

Fig. 2 — Probability density function of the phase of $s + n + i$ for various CIR values. (a) CNR = 10 dB, (b) CNR = 15 dB, (c) CNR = 20 dB, (d) CNR = 25 dB.

curves for representative CNR values. As the interference amplitude increases it is seen to control or to affect the shape of the curve to a greater degree. At high interference levels a saddle-like shape appears with peaks at roughly $\tan^{-1}b$, as one would expect in the absence of noise.

Since equation (13) is the probability density function of the angle of the complete receiver input, and since the probability of a symbol error is the probability that A lies outside the region $[-\pi/M, \pi/M]$ at t_0, we have

$$\mathrm{Pe} = \int_{-\pi}^{-\pi/M} f_A(\alpha)\, d\alpha + \int_{\pi/M}^{\pi} f_A(\alpha)\, d\alpha \tag{14}$$

which by symmetry is

$$\mathrm{Pe} = 2 \int_{\pi/M}^{\pi} f_A(\alpha)\, d\alpha. \tag{15}$$

Again, integral (15) was done numerically (a simple summation of the f_A data) for practical combinations of CNR, CIR, and for $M = 2, 3$, and 4. The results appear in Figs. 3–5.*

The above method, which employs two (rather simple) machine integrations, yields exact results but at the expense of not generating useful expressions for Pe. Therefore we now indicate one approach which yields Pe for $M = 2$, and bounds Pe for $M > 2$, as a convergent series. We begin by considering binary reception.

Referring back to Fig. 1, an error is made if $|\alpha| > 90°$ or, equivalently, if the resultant resides in the lower half plane $y < 0$. Then for fixed Φ,

$$\mathrm{Pe} \mid \Phi = (2\pi\sigma^2)^{-\frac{1}{2}} \int_{-\infty}^{0} \exp\left[-\frac{1}{2\sigma^2} (y - 1 - b\cos\phi)^2 \right] dy$$

$$= \tfrac{1}{2} \operatorname{erfc}\left(\frac{1 + b\cos\phi}{(2)^{\frac{1}{2}}\sigma} \right). \tag{16}$$

Averaging over the uniformly weighted Φ gives

$$\mathrm{Pe} = \frac{1}{\pi} \int_0^{\pi} \tfrac{1}{2} \operatorname{erfc}\left(\frac{1 + b\cos\phi}{(2)^{\frac{1}{2}}\sigma} \right) d\phi. \tag{17}$$

This integral, which is virtually the cumulative distribution function of a sine wave of amplitude b plus gaussian noise of variance σ^2

* The abscissa values are true carrier-to-noise power ratios, and are not adjusted to reconcile bandwidth to bit-rate differences. One may do this by subtracting 2 dB (3 dB) from the abscissa values for $M = 3(4)$.

(evaluated at -1), has been examined by Rice[4] and others. It can be evaluated by expanding the integrand in a Taylor series about $(2\sigma^2)^{-\frac{1}{2}}$ and then integrating term by term. If the interference is small, $b \ll 1$, only the first several terms need be retained for reasonable accuracy.

The Pe values obtained for Binary may be used to bound the symbol Pe for $M > 2$. The decision thresholds are at $\pm\pi/M$ for the M-ary receiver. The error region consists of the union of two half planes formed by the extended detector thresholds. The probability that the resultant

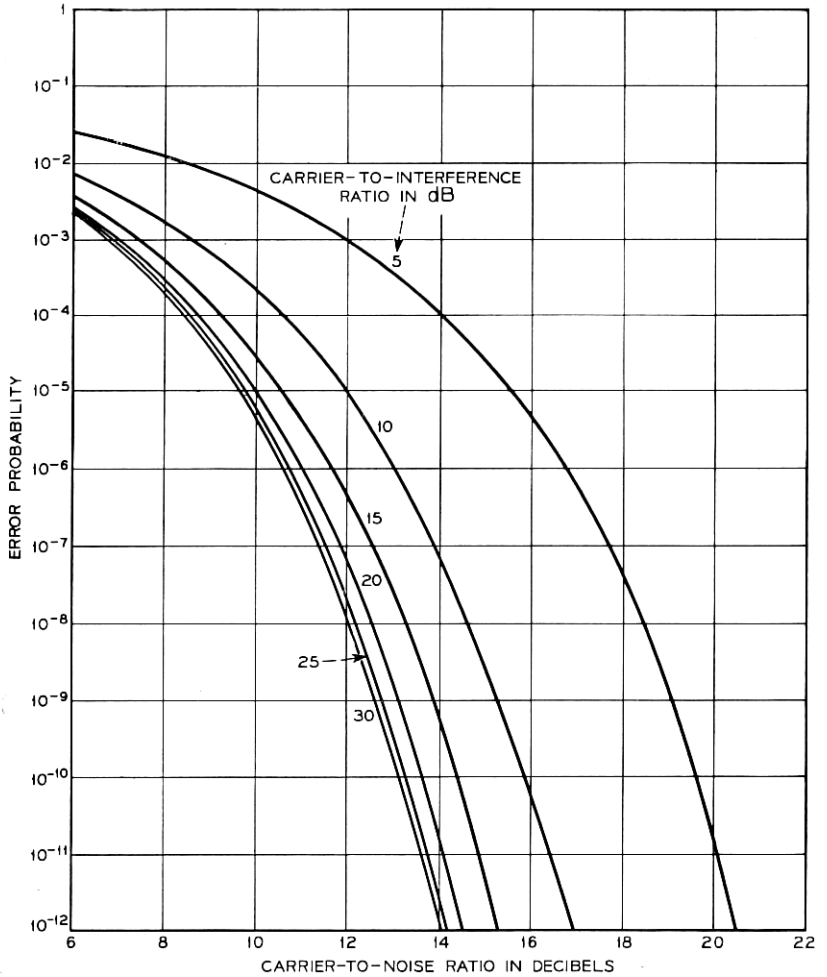

Fig. 3 — Binary ($M = 2$) Pe versus CNR. Coherent detection.

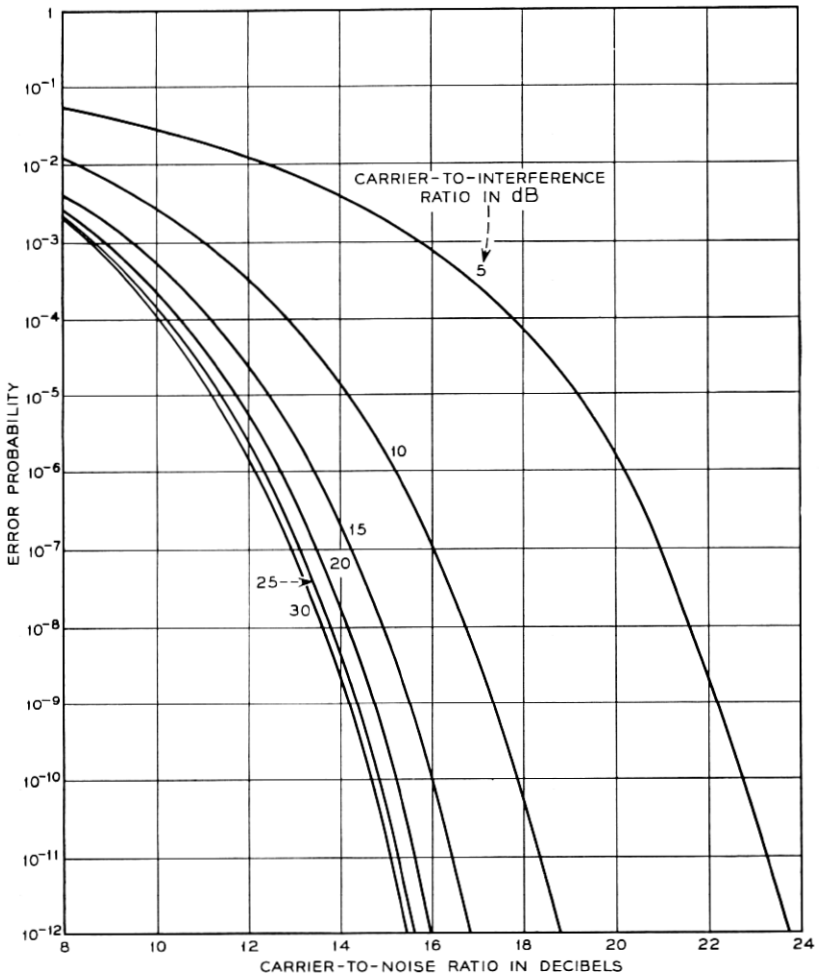

Fig. 4 — Ternary ($M = 3$) Pe versus CNR. Coherent detection.

phasor terminates in the error region, Pe, is thus bounded by the probability of terminating in either half plane. As M increases, the bound becomes a good approximation* because the size (hence the relative probability) of the doubly counted intersection decreases rapidly with M.[5] By symmetry, the probability of terminating in either half plane is twice that of one half plane.

* The approximation improves with CNR also.

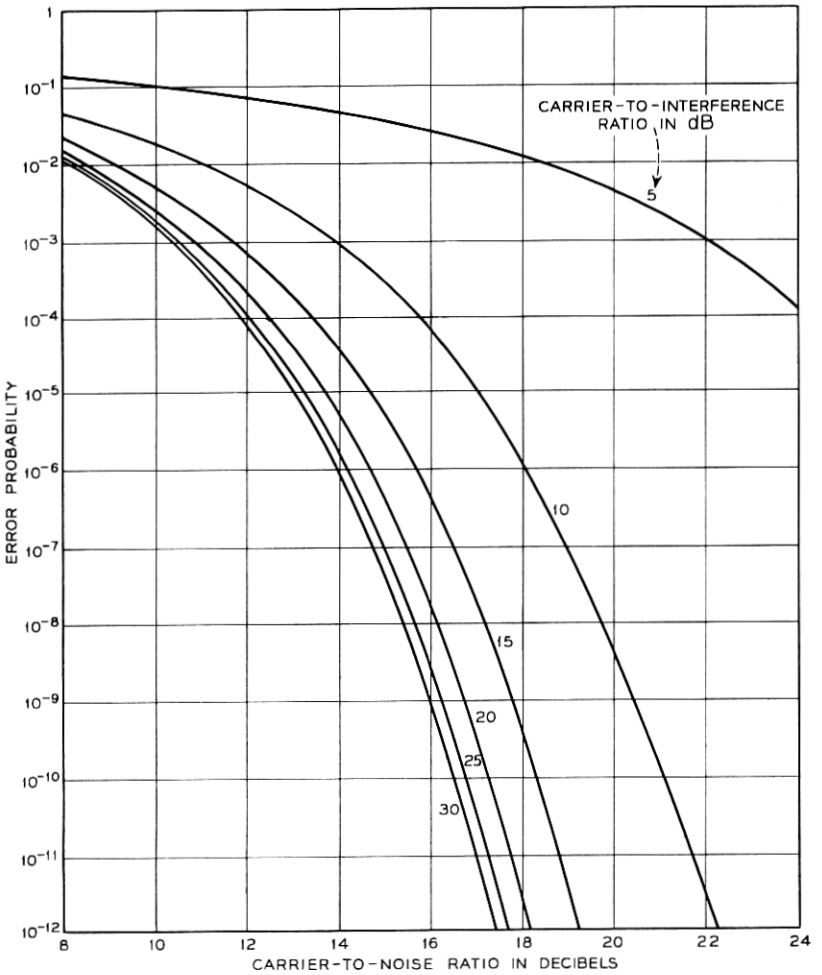

Fig. 5 — Quaternary ($M = 4$) Pe versus CNR. Coherent detection.

The probability of one half plane is related to the binary Pe very simply. The distance to the boundary from (0, 1) is sin (π/M). If now the interference phasor and noise phasor were scaled by the same factor, we see that the probability of the half plane is just the binary Pe with interference amplitude b sin (π/M) and noise variance $[\sigma \sin (\pi/M)]^2$.*

* The author is grateful to S. O. Rice for suggesting this notion.

Therefore we have the interesting relationship

$$\text{Pe}\left(M > 2,\ \sigma \sin \frac{\pi}{M},\ b \sin \frac{\pi}{M}\right) \leqq 2\ \text{Pe}\ (M = 2,\ \sigma, \pm b) \tag{18}$$

which means that twice a given binary Pe value is an upper bound (or approximation) to an M-ary Pe where the binary CNR and CIR values are each increased by $-20 \log \sin (\pi/M)$ dB.

IV. DIFFERENTIAL DETECTION—BINARY

This type of detection has become widely considered lately because it eliminates the requirement of phase synchronism between the transmitter and receiver. The price one pays for nonsynchronous detection, however, is poorer performance.

The analysis for differential detection is complicated by the fact that the phase reference, being the previous signal, is subject to the same corruptions as the present signal being phase detected. (For the noise-only case, an exact solution in closed form is available for binary, and good approximations exist for $M \geqq 4$.) We begin with an analysis for binary differential psk (d-psk), considering again a single CW interference in addition to noise, which yields in closed form both bounds on Pe and a good approximation.

We are concerned with the reception of two successive bauds, where the data is encoded in the phase change of the signal. Arbitrarily, let no phase change represent a "0" and a π phase change represent a "1." For convenience, we will refer to the signal during a baud interval as a "pulse" of carrier at a certain phase angle, although in a pure phase modulated (PM) system the signal would not consist of carrier pulses.

From previous assumptions, the noise corrupting each signal pulse acts independently; the interference at two adjacent sample times t_0 and $t_0 + T$ does not. This dependency may be summarized by an angle

$$\theta \equiv 2\pi(f_i - f_s)T$$

which is the relative phase slip of the interference from one sample instant to the next. Assume, for the present, that the interference modulation is absent.

We will use the same equally spaced detection thresholds as in the coherent psk analysis. Ignoring interference, the probability of error in d-psk is not data dependent because of obvious symmetries.

However, the addition of interference destroys that symmetry, and causes Pe to be strongly data dependent for a given θ. Fortunately, however, the error probability for only one symbol (that is, "0" or "1") needs to be found because the probability of error for the other symbol(s) is derived directly from it. An over-all probability of error is then found by averaging the individual symbol error probabilities with equal weighting.

Consider the transmission of a "0" whereby two carrier pulses of the same phase are sent. A "double exposure" phasor diagram, Fig. 6, pictures the signal, noise, and interference components at the two successive sample instants t_0 and $t_0 + T$. The interference at t_0 assumes an angle ϕ relative to the signal, where ϕ is random and uniformly distributed in $[0, 2\pi]$. At time $t_0 + T$ the interference has progressed to an angle $\phi + \theta$.

The noise phasor amplitudes are the random variables

$$U_d \equiv u(t_0), \quad V_d \equiv v(t_0), \quad U \equiv u(t_0 + T), \quad \text{and} \quad V \equiv v(t_0 + T) \tag{19}$$

which we recall are independent, equal variance, zero mean gaussians.

The two resultant phasors, Z and Z_d, are the actual phase discriminator inputs; the output being their phase difference, δ. Since a

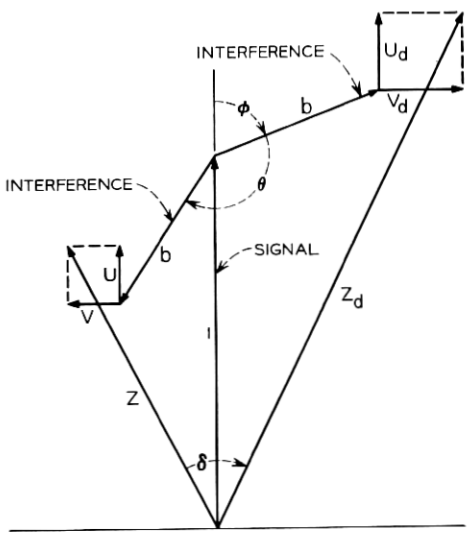

Fig. 6 — Signal, interference, and noise phasors at successive sample times t_0 and $t_0 + T$ for a transmitted "0."

"0" is transmitted, the probability of error is

$$\text{Pe} \mid \text{"0"} = \Pr\left\{ \mid \delta \mid > \frac{\pi}{2} \right\}, \qquad -\pi < \delta \leqq \pi \tag{20}$$

which is equivalent to $\Pr\{\cos \delta < 0\}$.

Also, because

$$\cos \delta = \frac{\text{Re}\,[ZZ_d^*]}{\mid Z \mid \mid Z_d \mid} \tag{21}$$

and the denominator is nonnegative, we have alternatively

$$\text{Pe} \mid \text{"0"} = \Pr\{\text{Re}\,[ZZ_d^*] < 0\}. \tag{22}$$

We now employ a technique used by Stein which leads to a closed form solution to equation (22).[6] Based on the simple identity

$$\text{Re}\,[ZZ_d^*] = \left| \frac{Z + Z_d}{2} \right|^2 - \left| \frac{Z - Z_d}{2} \right|^2 \tag{23}$$

we see that

$$\text{Pe} \mid \text{"0"} = \Pr\{\mid Z + Z_d \mid < \mid Z - Z_d \mid\} \tag{24}$$

For economy of notation we let

$$\begin{aligned} \Sigma &\equiv Z + Z_d = U + U_d + i(V + V_d) + C(\Sigma) \\ \Delta &\equiv Z - Z_d = U - U_d + i(V - V_d) + C(\Delta) \end{aligned} \tag{25}$$

where $C(\,)$ denotes the nonrandom components,* that is,

$$\begin{aligned} C(\Sigma) &= b[\sin \phi + \sin (\phi + \theta)] \\ &\quad + i\{2 + b[\cos \phi + \cos (\phi + \theta)]\} \\ C(\Delta) &= b[\sin (\phi + \theta) - \sin \phi] + ib[\cos (\phi + \theta) - \cos \phi]. \end{aligned} \tag{26}$$

Thus Σ and Δ are complex (two dimensional) random variables whose jointly gaussian orthogonal components have equal variance $2\sigma^2$. We are concerned with the magnitudes, $\mid \Sigma \mid$ and $\mid \Delta \mid$, often referred to as a Ricean random variable.

The probability density function (of $\mid \Sigma \mid$, for example) is the well known result for the envelope of sine wave plus noise[4]

$$f_{\mid \Sigma \mid}(r) = \frac{r}{2\sigma^2} \exp\left[- \frac{r^2 + \mid C(\Sigma) \mid^2}{4\sigma^2} \right] I_0\left[\frac{r \mid C(\Sigma) \mid}{2\sigma^2} \right]. \tag{27}$$

* θ is constant and we have conditioned the solution on ϕ.

Furthermore, $|\Sigma|$ and $|\Delta|$ are independent by the following argument. $U + U_d$ is independent of $V - V_d$. Consider $U + U_d$ and $U - U_d$. They are uncorrelated, hence independent, by virtue of their equal variance.

$$\langle[(U + U_d)(U - U_d)]\rangle_{av} = [U^2 - U_d^2] = 0 \tag{28}$$

Therefore all four random components of Σ and Δ are independent, from which the independence of $|\Sigma|$ and $|\Delta|$ follows.

The advantage of this approach is that equation (24), the probability that the amplitude of one complex gaussian (that is, a Ricean) exceeds another, is expressible in terms of the function[7]*

$$Q(A, B) \equiv \int_B^\infty \tau \exp\left(-\frac{A^2 + \tau^2}{2}\right) I_0(A\tau)\, d\tau. \tag{29}$$

One formulation is[8]

$$\Pr\{|\Sigma| < |\Delta|\} = \frac{1}{2}\left\{1 - Q\left[\frac{|C(\Sigma)|}{2\sigma}, \frac{|C(\Delta)|}{2\sigma}\right] + Q\left[\frac{|C(\Delta)|}{2\sigma}, \frac{|C(\Sigma)|}{2\sigma}\right]\right\}. \tag{30}$$

Evaluating the magnitudes of the means from equation (26),

$$\begin{aligned} |C(\Sigma)| &= 2\left[1 + 2b\cos\frac{\theta}{2}\cos\left(\phi + \frac{\theta}{2}\right) + b^2\cos^2\frac{\theta}{2}\right]^{\frac{1}{2}} \\ |C(\Delta)| &= 2b\sin\frac{\theta}{2}. \end{aligned} \tag{31}$$

We have thus far found Pe|"0" exactly, conditioned on the initial interference angle ϕ. The desired result is obtained by averaging equation (30) over ϕ. However, inserting equation (31) into equation (30) leaves an expression which offers little promise for analytically performing the integration. As an alternative, the integral is both approximated and bounded in what follows, thereby avoiding a machine integration.

The integration parameter ϕ appears in $|C(\Sigma)|$ but is not a factor of $|C(\Delta)|$. Then with the identification

$$\begin{aligned} B &\equiv |C(\Sigma)|/2\sigma \\ A &\equiv |C(\Delta)|/2\sigma \end{aligned} \tag{32}$$

* Q functions are tabulated, but not adequately in the argument ranges needed for these problems. Their usefulness lies in having good approximations which lead to easy machine calculations. See Ref. 8.

we are led to consider the behavior of the integrand

$$F(A, B) \equiv \tfrac{1}{2}[1 - Q(B, A) + Q(A, B)] \tag{33}$$

as a function of B only (fix A). Familiarity with $F(A, B)$ suggests that it is roughly exponential in $-B^2/2$.

To affirm this supposition we first show that

$$\frac{\partial F(A, B)}{\partial B} = -BK(A, B)F(A, B) \tag{34}$$

where $K(A, B)$ is bounded near 1:

$$1 \geqq K(A, B) \geqq 1 - \epsilon. \tag{35}$$

This approach is motivated by the recognition that if $F(A, B)$ could be approximated by an exponential in B^2, the integral of $F(A, B)$ over ϕ would be simple.

The derivation of equations (34) and (35) consists of elementary manipulations of the series and integral representations for $Q(A, B)$ which are given in Ref. 8. Henceforth, a prime designates partial differentiation with respect to B. For brevity, let

$$E \equiv \exp\left[-\frac{A^2 + B^2}{2}\right]. \tag{36}$$

Then using the series representations

$$Q(A, B) = E \sum_{m=0}^{\infty} \left(\frac{A}{B}\right)^m I_m(AB) \tag{37}$$

$$1 - Q(B, A) = E \sum_{m=1}^{\infty} \left(\frac{A}{B}\right)^m I_m(AB) \tag{38}$$

we see that

$$2F(A, B) = 2Q(A, B) - EI_0(A, B). \tag{39}$$

Then

$$2F'(A, B) = 2Q'(A, B) - EI_0'(AB) - E'I_0(AB) \tag{40}$$

$$= 2Q'(A, B) - EAI_1(AB) + BEI_0(AB). \tag{41}$$

Referring to the integral representation for the Q function we inspect

$$Q'(A, B) = -BEI_0(AB). \tag{42}$$

Therefore, from equations (42) and (41) we have

$$2F'(A, B) = -BE\left[I_0(AB) + \frac{A}{B} I_1(AB) \right]. \tag{43}$$

But from equations (37) and (38),

$$1 - Q(B, A) + Q(A, B) = E\left[I_0(AB) + 2 \sum_{m=1}^{\infty} \left(\frac{A}{B}\right)^m I_m(AB) \right]. \tag{44}$$

So that equation (34) is true for

$$K(A, B) = \frac{I_0(AB) + \left(\frac{A}{B}\right) I_1(AB)}{I_0(AB) + 2\left(\frac{A}{B}\right) I_1(AB) + 2 \sum_{m=2}^{\infty} \left(\frac{A}{B}\right)^m I_m(AB)}. \tag{45}$$

Since A, B, and the $I_m(x)$ are nonnegative the unity upper bound in equation (35) is obvious. For the lower bound, invert equation (45) and notice that

$$K(A, B)^{-1} \leqq 1 + 2 \sum_{m=1}^{\infty} \left(\frac{A}{B}\right)^m \frac{I_m(AB)}{I_0(AB)} \tag{46}$$

$$\leqq 1 + 2 \sum_{m=1}^{\infty} \left(\frac{A}{B}\right)^m \tag{47}$$

since the $I_m(x)$ decrease with the order m.

Referring to the definitions of equations (32) and (31) it can be shown that $A < B$ whenever $b < 1/(2)^{1/2}$, so that the summation converges for reasonable interference levels (CIR $>$ 3 dB). Then

$$K(A, B)^{-1} \leqq 1 + \frac{2A}{B - A} \tag{48}$$

so that

$$\epsilon \leqq \frac{2A}{B + A}. \tag{49}$$

In most cases $B \gg A$ so that $K(A, B)$ is near 1.

We now solve the linear, first order differential equation (34) to obtain

$$F(A, B) = \mathrm{Pe}_0 \exp\left[\int_{B_0}^{B} - \tau K(A, \tau)\, d\tau \right] \tag{50}$$

with initial data $F(A, B_0) = \mathrm{Pe}_0$. The above expression for $F(A, B)$

is exact. We now approximate the exp argument by approximating $K(A, B)$ with a constant K_0. Then we are able to carry out the integration in equation (50) to obtain

$$F(A, B) \approx \mathrm{Pe}_0 \exp\left[-\frac{K_0}{2}(B^2 - B_0^2)\right]. \tag{51}$$

We know the function at B_0, and we extrapolate to the function using an approximation of its derivative. Now the ϕ integration will range over some section of the exponentially varying $F(A, B)$ in equation (51) above. Because it is exponential, the significant contribution to the integral occurs over a relatively small range of B where $F(A, B)$ is near its maximum. This suggests that the initial data be specified at a maximum so that the approximation function is best in the important range of integration. Therefore we let

$$B_0 = B_{\min} \tag{52}$$

so that

$$\mathrm{Pe}_0 = F(A, B_0) \geqq F(A, B), \qquad 0 \leqq \phi \leqq 2\pi. \tag{53}$$

We notice from equation (31) that

$$B_{\min} = \frac{1}{\sigma}\left(1 - b\cos\frac{\theta}{2}\right) \tag{54}$$

and so

$$B^2 - B_0^2 = \frac{2b}{\sigma^2}\cos\frac{\theta}{2}\left[1 + \cos\left(\phi + \frac{\theta}{2}\right)\right]. \tag{55}$$

In addition, we slope-match at B_0, approximating $K(A, B)$ by $K_0 = K(A, B_0)$. From equation (45)

$$K(A, B_0) \approx \frac{1 + \left(\frac{A}{B_0}\right)\frac{I_1(AB_0)}{I_0(AB_0)}}{1 + 2\left(\frac{A}{B_0}\right)\frac{I_1(AB_0)}{I_0(AB_0)}}. \tag{56}$$

Inserting equation (55) into equation (51) and integrating,

$$\frac{1}{2\pi}\int_0^{2\pi} F(A, B)\, d\phi = F(A, B_0)\exp\left[-\frac{bK_0}{\sigma^2}\cos\frac{\theta}{2}\right] \cdot \int_0^{2\pi}\frac{d\phi}{2\pi}\exp\left[-\frac{bK_0}{\sigma^2}\cos\left(\phi + \frac{\theta}{2}\right)\right] \tag{57}$$

gives the desired result

$$\text{Pe} \mid \text{“0”} = \tfrac{1}{2}[1 - Q(B_0, A) + Q(A, B_0)] \cdot \exp\left[-\frac{bK_0}{\sigma^2}\cos\frac{\theta}{2}\right] I_0\left[\frac{bK_0}{\sigma^2}\cos\frac{\theta}{2}\right]. \tag{58}$$

Exact bounds are now easily obtained by bounding $K(A, B)$. With B_0 still chosen to be $B_{\min}$, clearly

$$\int_{B_0}^{B} -\tau K(A, \tau)\, d\tau \leqq \int_{B_0}^{B} -\tau K_{\min}\, d\tau = -\tfrac{1}{2}(B^2 - B_0^2)K_{\min} \tag{59}$$

where $K_{\min}$ is the minimum value of $K(A, B)$ in $[B_0, B]$. Similarly,

$$\int_{B_0}^{B} -\tau K(A, \tau)\, d\tau \geqq -\tfrac{1}{2}(B^2 - B_0^2)K_{\max}\,. \tag{60}$$

Therefore

$$F(A, B) \gtrless \text{Pe}_0 \exp\left[-\tfrac{1}{2}(B^2 - B_0^2)K_{\min}\right] \tag{61}$$

so that

$$\text{Pe} \mid \text{“0”}, \theta \lessgtr \text{Pe}_0 \exp\left[-K_{\min}\frac{b}{\sigma^2}\cos\frac{\theta}{2}\right] I_0\left[K_{\max}\frac{b}{\sigma^2}\cos\frac{\theta}{2}\right]. \tag{62}$$

The ratio of the bounds in equation (62) may be bounded in order to ascertain their closeness. We omit the cumbersome derivation, but state the result below.

$$\frac{\text{Upper Bound}}{\text{Lower Bound}} \leqq \left[\frac{\frac{1}{b} - \cos\frac{\theta}{2} + \sin\frac{\theta}{2}}{\frac{1}{b} - \cos\frac{\theta}{2} - \sin\frac{\theta}{2}}\right]^{0.65} \tag{63}$$

For CIR $\geqq$ 10 (15) dB, the ratio is less than 1.6 (1.25).

The symbol “1” is transmitted as two pulses of carrier 180° apart. Then correct reception results if $90° < |\delta| < 180°$. If an analysis quite similar to the preceding were carried out for this case, the resulting expressions would be identical with those above except that θ is replaced by $\pi - \theta$. It follows that

$$\text{Pe} \mid \text{“1”}, \theta = \text{Pe} \mid \text{“0”}, \pi - \theta. \tag{64}$$

We will elaborate on the relationship of Pe for the different data symbols in Section V.

Notice that Pe|"0" is symmetric in θ about 0 and π. The symmetry follows from the averaging of ϕ, and the insignificance of which of the two pulses occurs first as far as the detector is concerned.

Since the overall error probability

$$\text{Pe}\ (\theta) = \tfrac{1}{2}[\text{Pe} \mid \text{"1"}, \theta + \text{Pe} \mid \text{"0"}, \theta] \tag{65}$$

we use equation (64) to write

$$\text{Pe}\ (\theta) = \tfrac{1}{2}[\text{Pe} \mid \text{"0"}, \theta + \text{Pe} \mid \text{"0"}, \pi - \theta] \tag{66}$$

which is easily shown to be evenly symmetric about 0, π and $\pi/2$. We therefore need examine Pe only in the range $0 \leqq \theta \leqq 90°$.

Pe(θ) does vary considerably as seen in Fig. 7. Here the maximum and minimum values of Pe(θ), which happen to occur at $\pi/2$ and 0 respectively, are given for interesting combinations of interference and noise levels. To further illustrate the effects of interference, we present curves of decibel degradation versus θ in Fig. 8. Degradation is defined as the dB reduction in carrier-to-noise ratio which is allowed to maintain the same Pe after removing the interference.

Finally, consider an angle modulation impressed on the interference. This situation may be viewed simply as a time varying θ. Then one may average the Pe(θ) results given here over the variations of θ. If this is undesirable, the curves of Fig. 7 are certainly bounds on Pe averaged over the θ variation.

V. DIFFERENTIAL DETECTION—QUATERNARY

We now examine the effect of a single interference on a differentially detected quaternary (4-phase) signal. We will refer to the four symbols as "0", "1", "2", and "3", where the associated baud to baud phase shifts are 0, $\pi/2$, π, and $-\pi/2$ respectively. As before, the phase discriminator examines the two composite phasors, Z and Z_d, and reports their angle difference δ. The ordering of the bauds is important, since we must distinguish between $\delta = \pi/2$ and $\delta = -\pi/2$. The "0" symbol possesses the same symmetry as in the binary case; we therefore base the analysis on Pe|"0". Then in an analogous fashion we relate Pe|"0" to the probability of error for the other symbols.

In the binary case the receiver tested for the sign of Re $[ZZ_d^*]$. This test was transformable to a test between the amplitudes of two Ricean random variables, one which enjoys a closed form solution. Unfortunately, in the present case the test, which is for a "0"

$$\text{Pe} \mid \text{“0”} = \Pr\left\{\cos\delta = \frac{\text{Re}\,[ZZ_d^*]}{\mid Z \mid \mid Z_d \mid} \leqq \frac{(2)^{\frac{1}{2}}}{2}\right\}$$

is not known to be transformable to one which has a closed solution. On the other hand, we offer a very straightforward analysis which is exact and amenable to machine computation.

Figure 9 is a “double exposure” of the signal, noise, and interference components for a “0”. The two carrier pulses are, of course, coincident and lie along the reference axis. We recall that the angle of

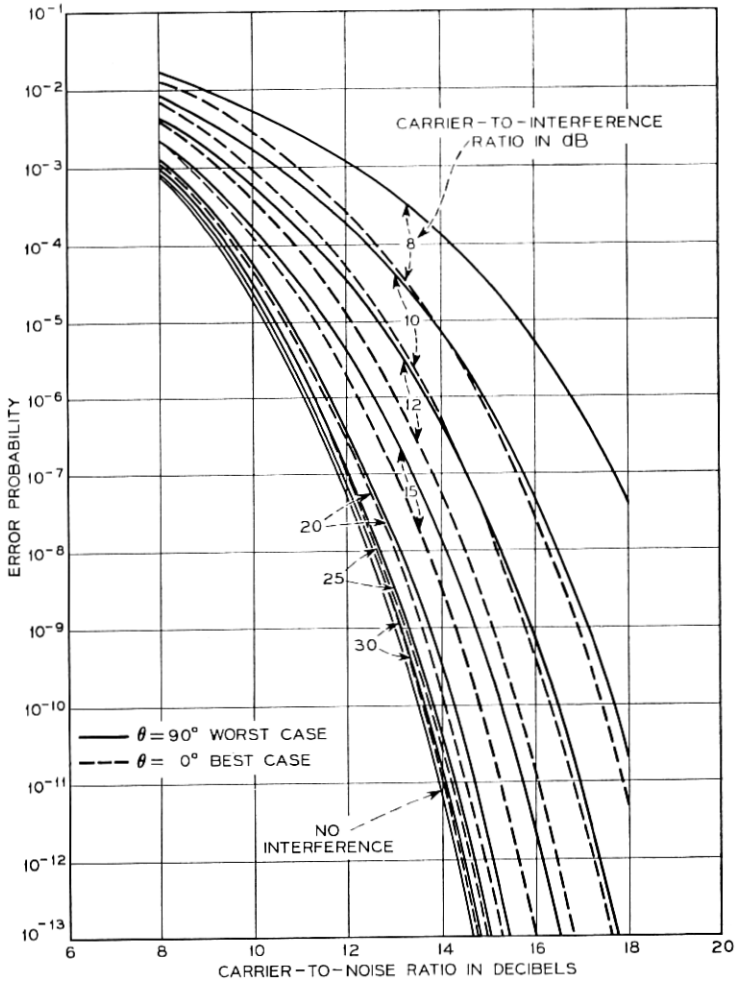

Fig. 7 — Binary Pe versus CNR. Differential detection.

the interference at t_0 is ϕ, and at $t_0 + T$ is $\phi + \theta$. We will again average over ϕ, leaving θ as a parameter.

At time t_0 the resultant of signal and interference, shown by a dashed line, has length W and angle ξ which by inspection are

$$W = (1 + b^2 + 2b \cos \phi)^{\frac{1}{2}} \tag{67}$$

$$\xi = \tan^{-1}\left[\frac{b \sin \phi}{1 + b \cos \phi}\right]. \tag{68}$$

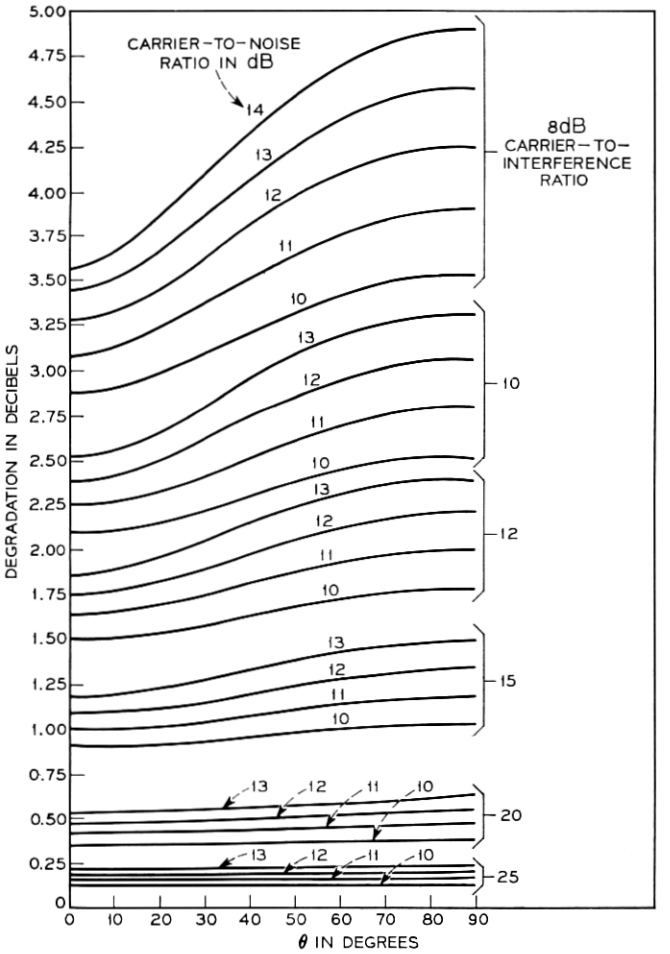

Fig. 8 — Degradation in CNR caused by interference versus θ for binary differential detection.

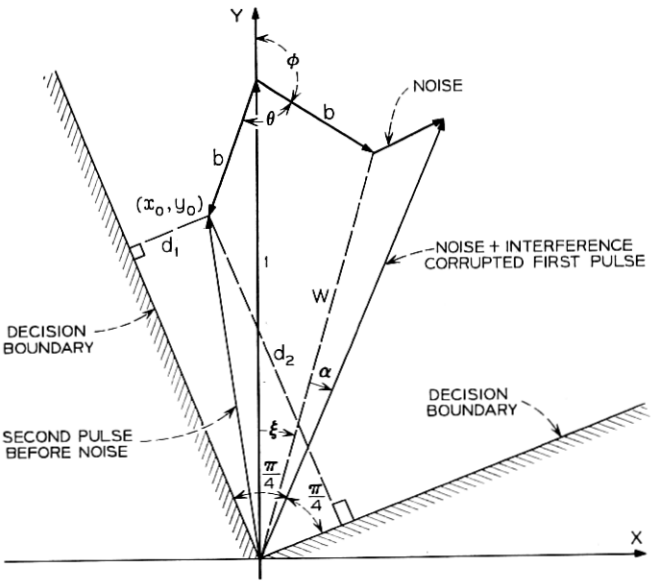

Fig. 9 — Phasor diagram for quaternary differential detection.

To the resultant of signal and interference adds a Rayleigh amplitude, uniform angle noise phasor. The resultant W is perturbed both in amplitude and angle by the noise. The resulting amplitude is unimportant, but the angle, $\xi + \alpha$, establishes the reference for detecting the second pulse. The probability density function of α is well known to be

$$f_\alpha(\alpha) = \frac{1}{2\pi} \exp(-\Psi)\{1 + \Psi^{\frac{1}{2}}\pi \cos\alpha \cdot \exp(\Psi \cos^2\alpha)[1 + \operatorname{erf}(\Psi^{\frac{1}{2}} \cos\alpha)]\} \tag{69}$$

where

$$\operatorname{erf}(x) \equiv \frac{2}{\pi^{\frac{1}{2}}} \int_0^x \exp(-u^2)\, du \tag{70}$$

is the usual error function integral and

$$\Psi = \frac{W^2}{2\sigma^2} \tag{71}$$

is the power ratio (signal plus interference)/noise.

At $t_0 + T$ the second pulse is examined. It is disturbed by interference to the point (x_0, y_0),

$$\begin{aligned} x_0 &= b \sin(\phi + \theta) \\ y_0 &= 1 + b \cos(\phi + \theta). \end{aligned} \tag{72}$$

The decoding region is a quarter plane bisected by the direction of the first pulse as shown by the orthogonal decision boundaries. The probability of correct reception is simply the probability that a random noise phasor originating at (x_0, y_0) will terminate inside this quadrant. Using the independent orthogonal phasor representation for noise, and choosing the components to lie alongside the perpendicular distances d_1 and d_2 from (x_0, y_0) to the boundaries, we write directly

$$1 - \text{Pe} \mid \text{“0”}, \phi, \alpha = \frac{1}{2}\left[1 + \operatorname{erf}\left(\frac{d_1}{2^{\frac{1}{2}}\sigma}\right)\right]\frac{1}{2}\left[1 + \operatorname{erf}\left(\frac{d_2}{2^{\frac{1}{2}}\sigma}\right)\right]. \tag{73}$$

Now using erf + erfc = 1 we have

$$\begin{aligned} \text{Pe} \mid \text{“0”}, \phi, \alpha = {} & \tfrac{1}{2}\operatorname{erfc}\left(\frac{d_1}{2^{\frac{1}{2}}\sigma}\right) \\ & + \tfrac{1}{2}\operatorname{erfc}\left(\frac{d_2}{2^{\frac{1}{2}}\sigma}\right) - \tfrac{1}{4}\operatorname{erfc}\left(\frac{d_1}{2^{\frac{1}{2}}\sigma}\right)\operatorname{erfc}\left(\frac{d_2}{2^{\frac{1}{2}}\sigma}\right). \end{aligned} \tag{74}$$

The distances d_1 and d_2 may be verified to be

$$\begin{aligned} d_1 &= -y_0 \sin\left(\alpha + \xi - \frac{\pi}{4}\right) + x_0 \cos\left(\alpha + \xi - \frac{\pi}{4}\right) \\ d_2 &= y_0 \sin\left(\alpha + \xi + \frac{\pi}{4}\right) - x_0 \cos\left(\alpha + \xi + \frac{\pi}{4}\right) \end{aligned} \tag{75}$$

such that they take the positive sign if (x_0, y_0) lies on the correct reception side of the respective boundary.

Eliminating the ϕ and α dependency results in a finite limits double integral

$$\text{Pe} \mid \text{“0”} = \int_0^{2\pi} \frac{d\phi}{2\pi} \int_{-\pi}^{\pi} f_\alpha(\alpha)\, \text{Pe} \mid \text{“0”}, \phi, \alpha \, d\alpha \tag{76}$$

which was machine evaluated.

The relationship between Pe | “0” and the other symbols is easily demonstrated graphically. Figure 10 is a phasor diagram illustrating a typical noise and interference corrupted first pulse, and the four

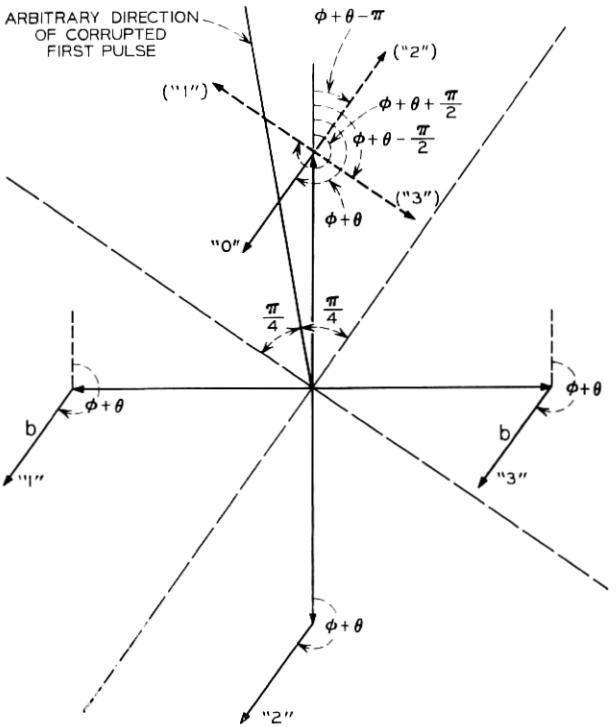

Fig. 10 — The relationship of $Pe|\theta$ for the individual symbols.

possible positions of the pre-interference second pulse. Decoding quadrants determined by the angle of the first pulse are shown by dashed lines. Adding to each of the possible second pulse carrier phasors, which correspond to the four data symbols, is an interference phasor having some angle $\phi + \theta$.

If a "0" had been sent, the probability of error conditioned on the present geometry (that is, the values of ϕ, α, and θ) is the probability that a noise phasor originating at the tip of the solid interference phasor (labeled "0") terminates outside the "0" quadrant. This probability is a function of σ and the distances from the tip of the interference phasor to the boundaries.

Now assume that a "3" had been sent instead. The associated second carrier pulse is shifted clockwise by $\pi/2$, but the interference phasor at $t_0 + T$ is still at $\phi + \theta$ relative to the diagram reference. Returning to the "0" quadrant, consider an interference phasor hav-

ing the angle $\phi + \theta - \pi/2$, shown by the dashed line labelled "3". It is apparent (and trivial to show) that the distances of the dashed "3" phasor to the "0" quadrant boundaries are identical with the distances of the actual "3" interference phasor to the "3" quadrant boundaries. We conclude, therefore, that

$$\text{Pe} \mid \text{“3”}, \phi, \alpha, \theta = \text{Pe} \mid \text{“0”}, \phi, \alpha, \theta - \frac{\pi}{2}. \tag{77}$$

Now integrating both sides of the equality over all ϕ, α yields the desired relationship

$$\text{Pe} \mid \text{“3”}, \theta = \text{Pe} \mid \text{“0”}, \theta - \frac{\pi}{2}. \tag{78}$$

Similarly we have

$$\text{Pe} \mid \text{“2”}, \theta = \text{Pe} \mid \text{“0”}, \theta - \pi \tag{79}$$

$$\text{Pe} \mid \text{“1”}, \theta = \text{Pe} \mid \text{“0”}, \theta + \frac{\pi}{2} \tag{80}$$

so that the average symbol error probability becomes

$$\text{Pe}(\theta) = \frac{1}{4}\left[\text{Pe} \mid \text{“0”}, \theta + \text{Pe} \mid \text{“0”}, \theta - \frac{\pi}{2} + \text{Pe} \mid \text{“0”}, \theta + \frac{\pi}{2} + \text{Pe} \mid \text{“0”}, \theta - \pi\right] \tag{81}$$

which is solely in terms of Pe | "0".

Notice that equation (79) is exactly the result obtained for a "1" in binary. This is not surprising, since a "2" constitutes a 180° phase shift of the second pulse. In fact, the arguments relating to Fig. 10 may be generalized for an M-phase d-psk signal with a "J" symbol phase shift of $(2\pi J)/M$, to be

$$\text{Pe} \mid \text{“}J\text{”}, \theta = \text{Pe} \mid \text{“0”}, \theta + \frac{2\pi J}{M}. \tag{82}$$

Averaging over the symbols in equation (81) produces a $\text{Pe}(\theta)$ which is evenly symmetric about 0, $\pi/4$, $\pi/2$, . . . ; points half as far apart as in binary. Also, while Pe|"0" still varies over a considerable range, when four symbols are averaged instead of two the range of $\text{Pe}(\theta)$ is significantly decreased. This is evidenced by the numerical results plotted in Fig. 11. Again, the solid and dashed lines represent

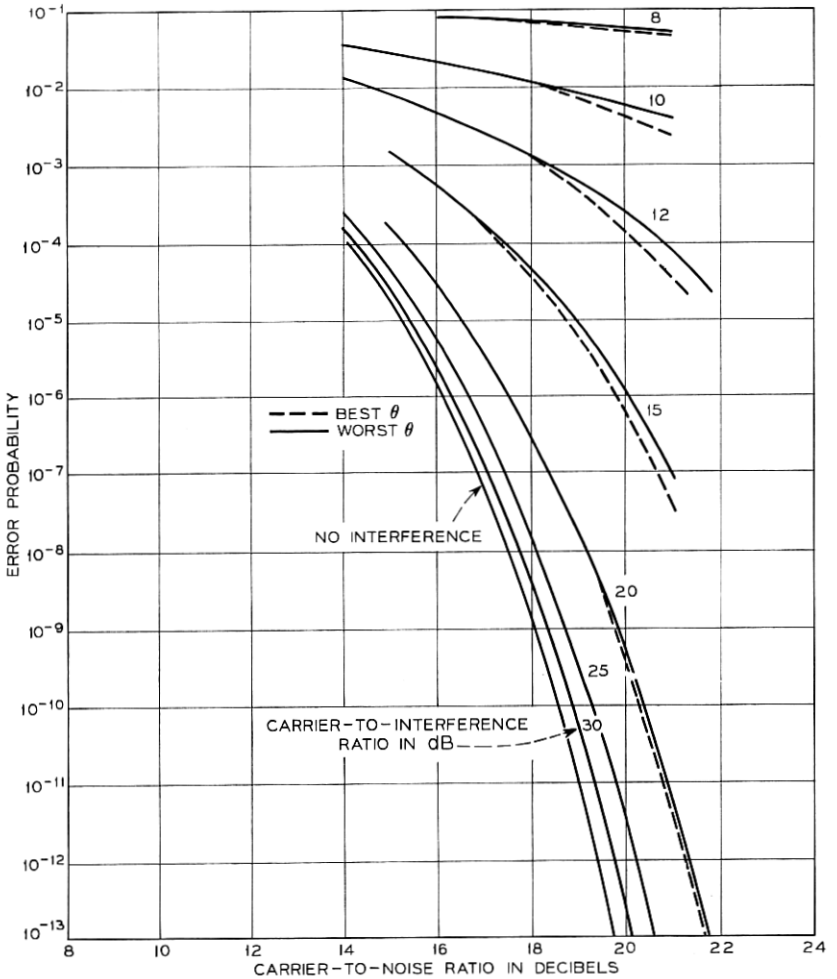

Fig. 11 — Quaternary symbol Pe versus CNR. Differential detection.

maximum and minimum values of the symbol Pe. The values of θ which correspond to the maximum and minimum are not the same for all noise and interference level combinations. However, $\mathrm{Pe}(\theta)$ is generally lowest near 0, $\pi/2$, π . . . and highest near $\pi/4$, $3\pi/4$, . . . , and so on.

Since $\mathrm{Pe}(\theta)$ fluctuates less severely for quaternary, it is more meaningful to average over θ. This was done, and the average used as a base for computing the degradation curves of Fig. 12.

VI. DIFFERENTIAL DETECTION — M > 4

For large M systems, for example $M \geqq 8$, we compute the average error probability

$$\mathrm{Pe} = \frac{M}{\pi} \int_0^{\pi/M} \mathrm{Pe}\,(\theta)\, d\theta \tag{83}$$

assuming now that θ is a uniformly distributed random variable. Because of the rapidly diminishing θ dependency noted in Section V, the average over θ is a useful measure of error performance. The choice of a uniform distribution for θ allows an approach which relies on the previously obtained $f_A(\alpha)$ data, rather than finding $\mathrm{Pe}(\theta)$ and then integrating.

Let the interference phase angles at t_0 and $t_0 + T$ be random variables Φ and $\Phi + \Theta$, respectively. We first note that the sum $\Phi + \Theta$ modulo 2π is uniformly distributed since Φ (or Θ) is uniform. Hence both interference angles, Φ and $\Phi + \Theta$, are uniformly distributed. Furthermore, since for any $\Phi = \phi$ the sum $\phi + \Theta$ (modulo 2π) is uniform, we conclude that Φ and $\Phi + \Theta$ are independent. The adjacent interference angles then are independent; and consequently the phase angle, A, of $s + n + i$ is independent from sample to sample.

We therefore obtain the probability density function of the differ-

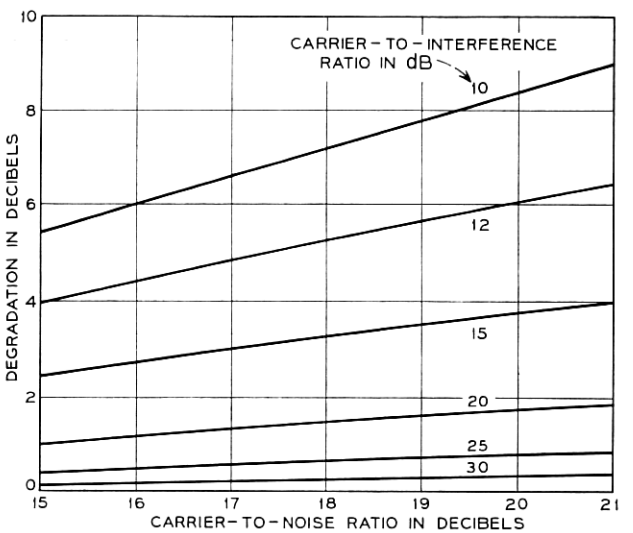

Fig. 12 — Degradation in CNR caused by interference for quaternary differential detection.

ence angle $\delta = A(t_0 + T) - A(t_0)$ as the modulo 2π convolution of $f_A(\alpha)$ with itself. Then the integral of the probability density function of δ over $|\delta| > (\pi/M)$ yields Pe. Numerical results were obtained in this fashion for $M = 4$, 8, and 16. The $M = 4$ data was in excellent agreement with Fig. 11. Pe for $M = 8$ and $M = 16$ is displayed in Fig. 13. When $b > \sin(\pi/2M)$ the interference alone can exceed the thresholds and cause errors. This is seen as a Pe floor for low CIR

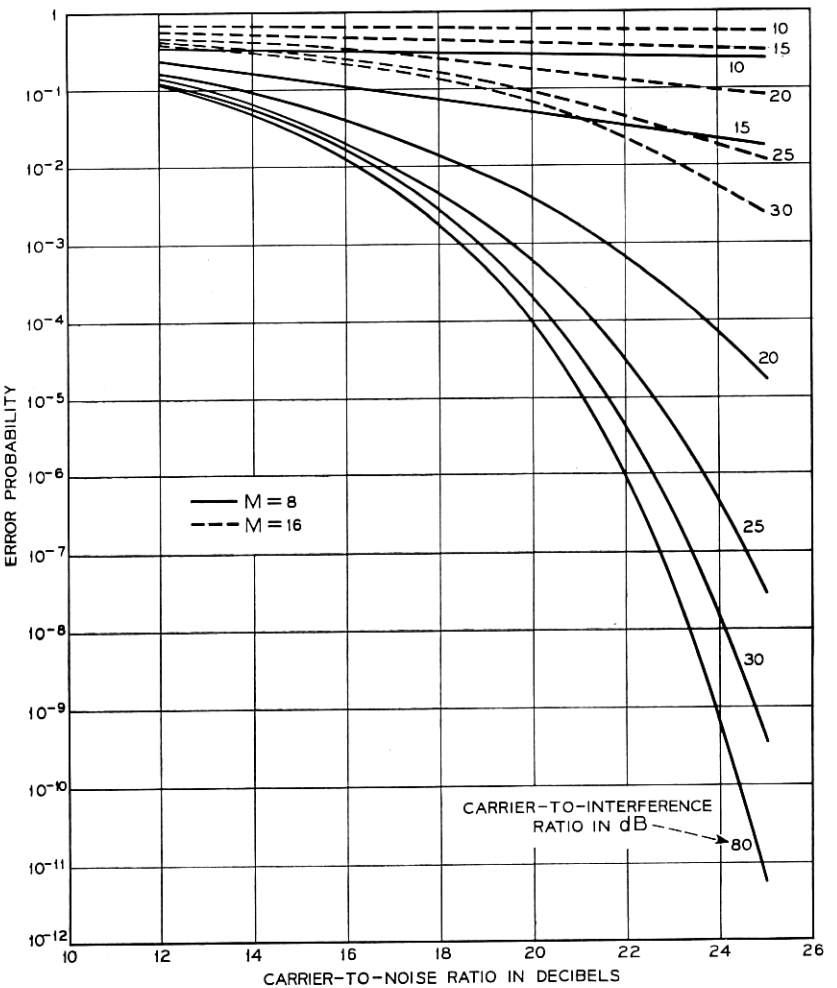

Fig. 13 — Symbol Pe versus CNR for 8 and 16 phase differential detection.

values; increasing CNR does not cause Pe to tend toward zero.

Finally, we remark that the averaging of Pe over the M symbols was implicitly done in the θ averaging. We see from equation (82) that all symbols have equal error probability when θ is uniformly distributed.

VII. SUMMARY AND CONCLUSIONS

We have evaluated the symbol error probabilities for both coherent and differential detection of low M psk signals in the presence of interference. The effect of the interference is readily observed in the curves of Figs. 3–5, 7, 11, and 13. Although the increase in Pe resulting from interference is large, it is considerably less than if the interference were replaced by gaussian noise of the same power, especially at low Pe levels.

Comparing Figs. 3, 4, and 5, we see that vulnerability increases with M. That is, at a given CNR, the Pe is raised least for $M = 2$ and greatest for $M = 4$ by the addition of interference. For example, without interference the error performance of $M = 2$ versus $M = 4$ differs by 3 dB. When a -10 dB interferer is added, it differs by approximately 5 dB, indicating a 2 dB CNR penalty for equal *Pe* values.

Drawing comparisons between coherent and differential detection reveals that differential detection clearly suffers more degradation. Binary differential, however, performs about as well with interference at optimum θ values as does binary coherent. This is in contrast with the performance disparity between the two $M = 4$ systems. With a -10 dB interference, differential detection suffers a degradation ranging from 5½ to 8 dB; coherent detection is degraded only 4 to 4½ dB for the same CNR range.

We use degradation rather than the raw Pe versus CNR curves to make the above comparisons because of the inherent difference in performance between differential and coherent psk for noise alone. That is, the degradation comparisons automatically reconcile any disparities in the noise-only performances of the various systems.

REFERENCES

1. Davenport, W. B. and Root, W. L., *Random Signals and Noise,* New York: McGraw-Hill, 1958, pp. 158–159.
2. Papoulis, A., *Probability, Random Variables and Stochastic Processes,* New York: McGraw-Hill, 1965, pp. 182–183.
3. Scire, F. J., "A Probability Density Function Theorem for the Modulo y Values of the Sum of Two Statistically Independent Processes," Proc. IEEE, *56,* No. 2 (February 1968), pp. 204–205.

4. Rice, S. O., "Statistical Properties of a Sine Wave Plus Random Noise," B.S.T.J., *27*, No. 1 (January 1948), pp. 109–114.
5. Arthurs, E. and Dym, H., "On the Optimum Detection of Digital Signals in the Presence of White Gaussian Noise—a Geometric Interpretation and a Study of Three Basic Data Transmission Systems," IRE Trans. on Communication Systems, *CS-10*, No. 4 (December 1962), pp. 336–372.
6. Stein, S., "Unified Analysis of Certain Coherent and Noncoherent Binary Communications Systems," IEEE Trans. on Information Theory, *IT-10*, No. 1 (January 1964), pp. 43–51.
7. Marcum, J. I., "Tables of the Q Function," Rand Corporation Memorandum RM-399 (January 1950).
8. Schwartz, M., Bennett, W. R., and Stein, S., *Communication Systems and Techniques*, New York: McGraw-Hill, 1966, Appendix A.